

# **A Directional Glide Path**

By

Thomas H Bottoms

Henry C. Hurley

Lawrence N Spinner

John W Watt

Electronics Division

**TECHNICAL DEVELOPMENT REPORT NO 336**



**CIVIL AERONAUTICS ADMINISTRATION  
TECHNICAL DEVELOPMENT CENTER  
INDIANAPOLIS, INDIANA**

**February 1958**

U. S. DEPARTMENT OF COMMERCE  
Sinclair Weeks, Secretary

CIVIL AERONAUTICS ADMINISTRATION  
James T Pyle, Administrator  
D. M. Stuart, Director, Technical Development Ce

#### TABLE OF CONTENTS

	Page
SUMMARY	1
INTRODUCTION	1
THEORY OF OPERATION	2
TEST RESULTS	12
THE MONITORING SYSTEM	15
CONCLUSIONS	22

This is a technical information report and does not  
necessarily represent CAA policy in all respects

## A DIRECTIONAL GLIDE PATH\*

### SUMMARY

This report presents the theory of operation and test results of an instrument landing system glide path and associated monitor identified as the directional glide path. It was developed at the Civil Aeronautics Administration Technical Development Center for the specific purpose of producing a straight path at sites where this was not possible, because of rough terrain, with either the equisignal or the null-reference glide paths. A directional glide path was installed and successfully operated at the Kanawha County Airport, Charleston, West Virginia, where the terrain is very rough.

### INTRODUCTION

The glide path is that part of the Civil Aeronautics Administration (CAA) Instrument Landing System (ILS) which provides the pilot with vertical guidance during an instrument approach. The assigned frequency spectrum, 328.6 to 335.4 Mc, accommodates 20 channels spaced 0.3 Mc.

A transmitter on the ground near the approach end of the runway energizes an antenna system, from which a carrier and 90-cycle-per-second (cps) and 150-cps sidebands are radiated. The system is so arranged that on-path is characterized by a carrier modulated with equal amounts of 90- and 150-cps energy. Below path, 150-cps modulation predominates, and above path, 90-cps modulation predominates.<sup>1</sup>

The airborne equipment, comprised of an antenna, receiver, and indicator, presents an indication which is a function of difference in depth of modulation (DDM). Since on-path is characterized by an r-f carrier modulated by equal amounts of 90- and 150-cps energy, the indicator is centered when the aircraft is on path. When the aircraft is above path, the indicator deflects downward to command fly down and vice versa when the aircraft is below path.<sup>2</sup>

Several types of antenna systems have been developed to produce a glide path. The field patterns of the antenna systems in current use depend on ground reflections to produce a straight path at the proper angle. For the production of a straight path, it is necessary that the terrain in the vicinity of the antenna system be reasonably flat and level. At sites where the terrain either rises or falls abruptly near the approach end of the runway, irregularities in the path result. In the directional glide path, the path is formed by a system which does not depend on ground reflections for its pattern formation.

Since the glide path is used by the pilot to establish his rate of descent and as a guide to the point of contact during the critical operation of landing, it is of extreme importance that a monitor be associated with the glide path system which will provide an alarm when any probable combination of malfunctioning of the system occurs. It must be accepted that perfect monitoring (the detection of every conceivable combination of malfunctioning) is practically impossible to attain. This is especially true when one considers the rather unlikely simultaneous occurrences of compensating errors. A good monitor will detect all of the likely malfunctions and a very large number of unlikely ones in addition. These include

---

\*Manuscript submitted for publication December 1957

<sup>1</sup>R. A. Hampshire and B. V. Thompson, "ILS-2 Instrument Landing Equipment," Electrical Communications, Vol. 27, No. 2, June 1950.

<sup>2</sup>For a more complete discussion of the operation of the glide path, the reader is referred to "The CAA Instrument Landing System," by Peter Caporale, Electronics, February and March, 1945.

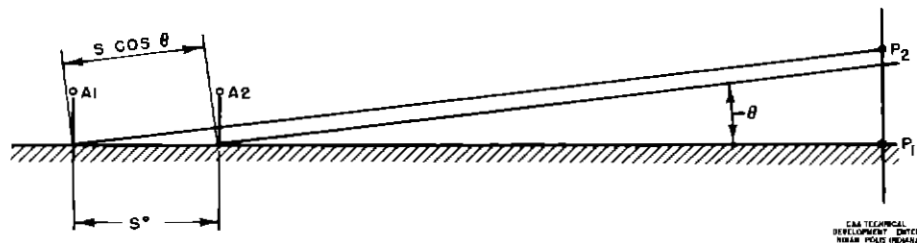


Fig 1 Geometry of Path Generation

failure within the monitoring system itself, which means that the monitoring circuitry must be as inherently fail-safe in nature as possible. Test results with the monitor developed for the directional glide path and described in this report indicate that it satisfies these requirements.

### THEORY OF OPERATION

Consider an arrangement of two dipoles A1 and A2, mounted approximately one wavelength above the ground and spaced "s" electrical degrees as shown in Fig 1. If it is assumed that the dipoles are fed inphase, then at a point P1 located at ground level, the instantaneous phase of the r-f field which arrives from A1 will be delayed with reference to the instantaneous phase of the r-f field arriving from A2 by "s" electrical degrees. If we consider point P2, a point some distance above ground, the phase delay will be less than "s" electrical degrees. It will simplify studying this phase change if the assumption is made that the energy arriving at P2 travels from the source in parallel rays as shown in Fig 1. This assumption will result in a negligible error if point P2 is at a distance from the midpoint between A1 and A2 which is very much greater than the spacing between A1 and A2. At

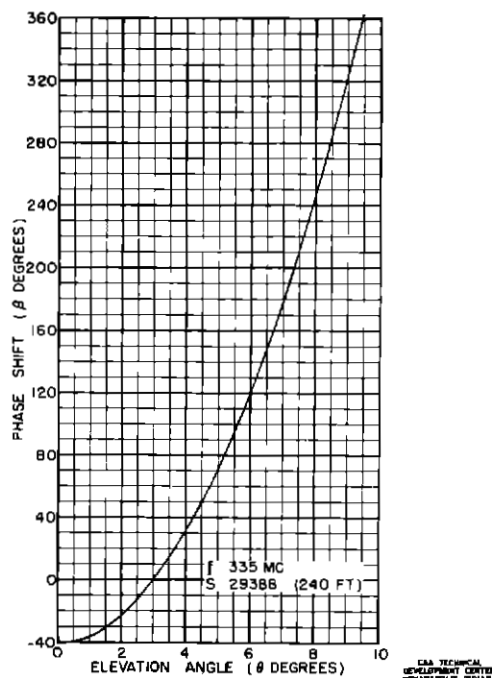


Fig 2 Phase Difference Versus Elevation Angle

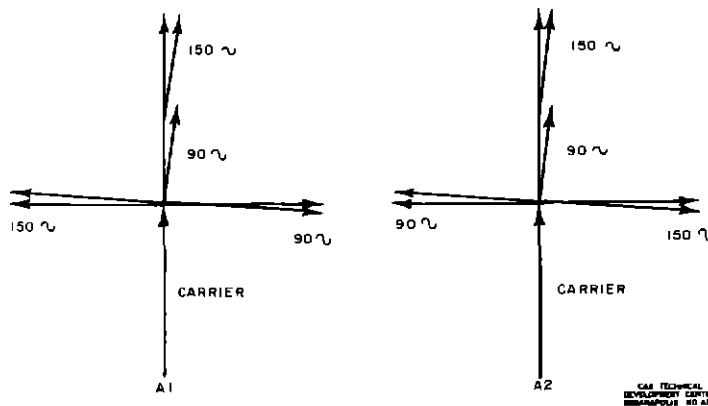


Fig 3 Vectorial Representation of R-F Fields

point P2 at an angle of  $\theta$ , the phase delay has decreased from "s" degrees to  $(s \cos \theta)$  degrees. Stated another way, when point P moves in elevation to increase the angle  $\theta$ , the phase of the r-f field arriving from A1 advances with respect to the phase of the r-f field arriving from A2.

It will be helpful to consider in somewhat more detail the rate and magnitude of the phase change in the vicinity of  $3^\circ$  elevation and for a spacing between A1 and A2 of 240 feet, or  $29388^\circ$  at 335 Mc. Dipoles A1 and A2 are energized separately and the initial phase can be fixed arbitrarily at any value. Assume that the initial phasing of the feed lines supplying A1 and A2 is adjusted to cause the r-f fields to arrive inphase at P when this point is on path angle ( $3^\circ$ ). Figure 2 shows how the phase difference between the r-f fields arriving at P changes as  $\theta$  varies. For constructing the graph, the phase of the r-f field arriving from A2 was used as a reference. If the spacing between A1 and A2 was increased, a greater phase change for a given change in  $\theta$  would result. It will be shown later that this offers a means for controlling course width.<sup>3</sup>

Now consider the vector character of the energy fed to A1 and A2. Referring to Fig 3, the field at point P is the vector sum of the two field components from A1 and A2. It will be observed that the sideband vectors of these two components are positioned differently. If the feed lines supplying the energy to A1 and A2 are independent, the initial phasing can be adjusted to cause the two components of the r-f field to arrive inphase at a point P located on a line corresponding to path angle. The vector sum of the field components contributed by A1 and A2, when they arrive inphase, is shown in Fig 4A. It is seen that the resultant is comprised of a carrier modulated equally with 90 and 150 cps. The response of a standardized glide path receiver to this input signal will be a centered pointer on the course deviation indicator (CDI) which the pilot interprets as on path.

It was shown previously that when point P moves in elevation so as to increase the angle  $\theta$ , the phase difference of the two field components arriving at P decreases. This is equivalent to saying that when the aircraft moves from a position on path to a position above path, the component of the r-f field associated with A1 advances in phase with respect to the field component from A2. Consider the case where the point P, that is, the aircraft, moves sufficiently above path to cause a phase advance of  $90^\circ$ . Reference to Fig 4B shows that this condition exists at an elevation angle of  $5.4^\circ$ . Figure 4B shows the relative phasing of the r-f field as it arrives at the aircraft and also the resultant of the two field components. The figure shows that the resultant comprises a carrier modulated at 90 cps only since the 150-cps sidebands cancel. A standardized glide path receiver will respond to this signal by indicating fly-down to the pilot.

---

<sup>3</sup>Course width - The course width above path is that angular displacement from path angle at which full-scale fly-down indication is obtained. Similarly the course width below path is that angular departure from on path at which full-scale fly-up indication is obtained. Total course width is the sum of the angular displacement above and below path at which full-scale indications are obtained. Unless otherwise stated, a reference to course width implies total course width.

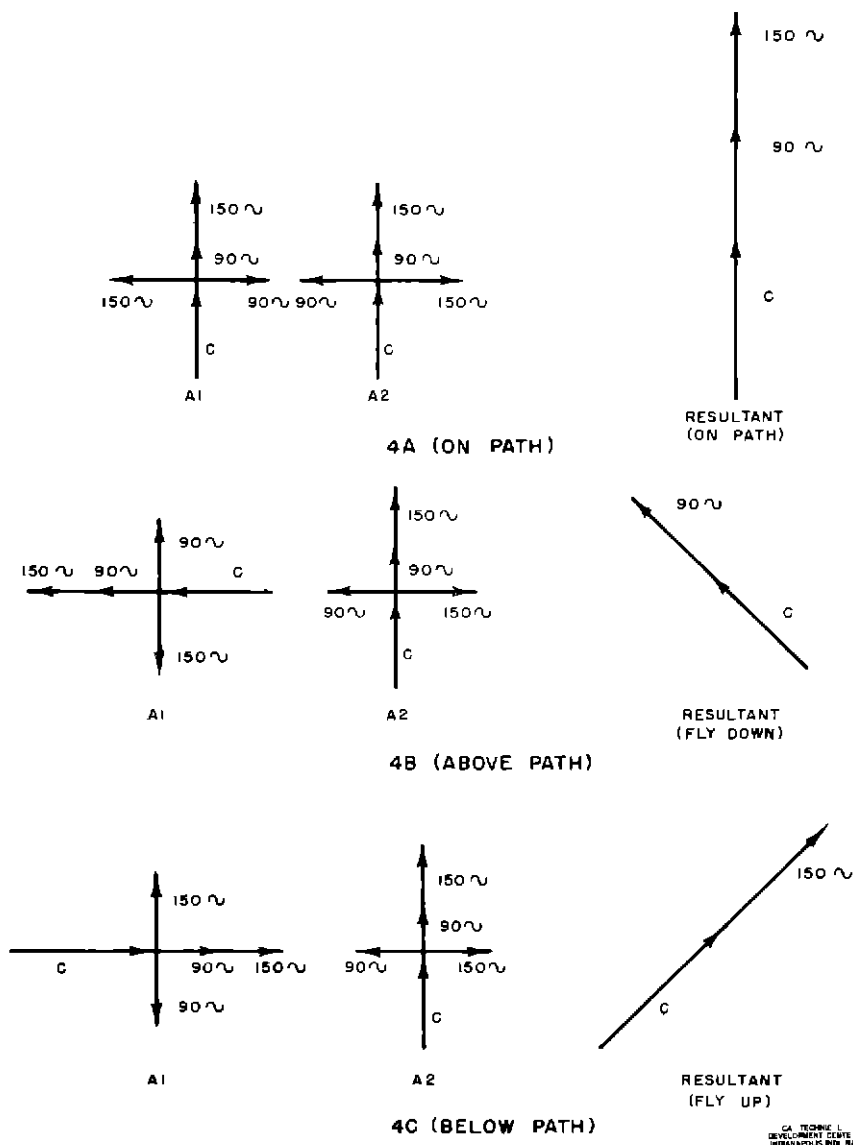


Fig 4 Vectorial Representation of R-F Fields at Different Elevations

By similar reasoning it can be shown that when the point P, or the aircraft, drops sufficiently below path to cause a  $90^\circ$  phase change, the 90-cps sidebands cancel and the resultant field arriving at the aircraft antenna will be a carrier modulated at 150 cps only, Fig 4C. The CDI will indicate fly-up, since the aircraft is below path. The displacements above and below path where a  $90^\circ$  phase shift occurs were chosen to illustrate the behavior of the directional glide path because these two positions are the special conditions for which either the 90-cps or the 150-cps sideband vanishes, as is shown by the vector diagram. Actually, for the case of a  $3^\circ$  glide path, the point P could not be moved sufficiently below path to cause a  $90^\circ$  phase change as can be seen from the graph in Fig 2. Also, it should be noted that a  $90^\circ$  phase shift produces maximum DDM and consequently, maximum displacement on the CDI. Vector diagrams could be constructed for angular departures from path of less than that necessary to produce a  $90^\circ$  phase change, which would show that as the point P departs from the on-path position, a progressive change in DDM occurs, and that this change is nearly linear in the region near path angle. Figure 5 shows a graph of DDM versus angular departure from path, for a path angle of  $3^\circ$ , carrier frequency of 335 Mc, and a

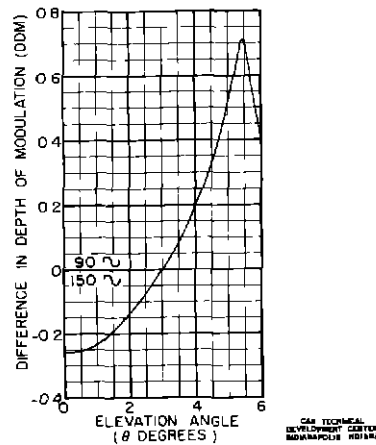


Fig 5 Difference of Depth of Modulation Versus Elevation Angle

spacing between A1 and A2 of 29388 electrical degrees. The relation between DDM and CDI deflection is shown in Fig 6. The indicator is illustrated in Fig 7. Full-scale deflection obtains for a current of 150 microamperes.

The simple arrangement of an end-fire array of two radiating elements described above would satisfy the requirements for vertical guidance if its use were confined to flight in a vertical plane which includes the centerline of the array. However, this would not constitute an acceptable glide path.

Consider the behavior of the system just described in three-dimensional space. Assume that point P is located in the vertical plane at an elevation angle  $\theta$  and that the initial phasing is such that the two separate components of the r-f field from A1 and A2 arrive in phase at a point located on path. It was shown that as the point P moves above path, a phase advance results and this produces a fly-down indication. As point P moves in azimuth at a constant elevation angle, a phase advance occurs also and this, too, will result in a fly-down indication.

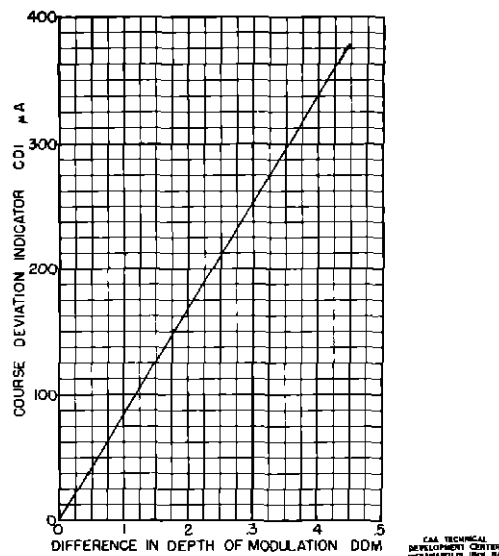
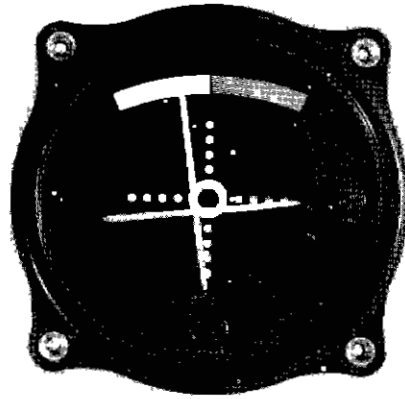
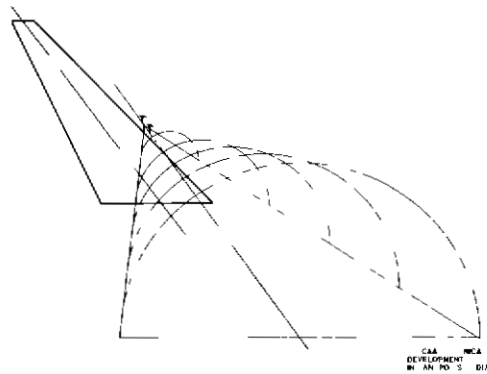


Fig 6 Course Deviation Indicator Versus Difference of Depth of Modulation Conversion Chart



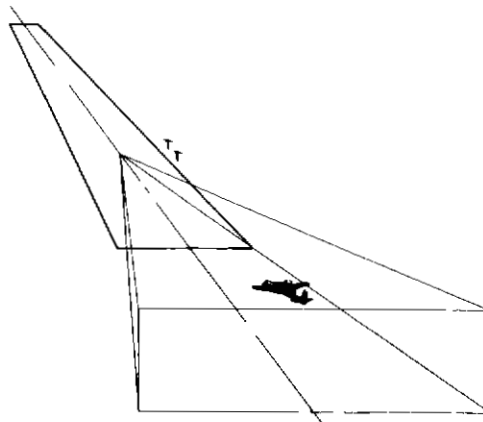
CAA  
F. ELLIP  
MANPOUS DIA

Fig 7 Course Deviation Chart



CAA  
DEVELOPMENT  
MANPOUS DIA

Fig 8 Pictorial Representation of Simple Directional Glide Path



CAA  
DEVELOPMENT  
MANPOUS DIA

Fig 9 Pictorial Representation of ILS Approach



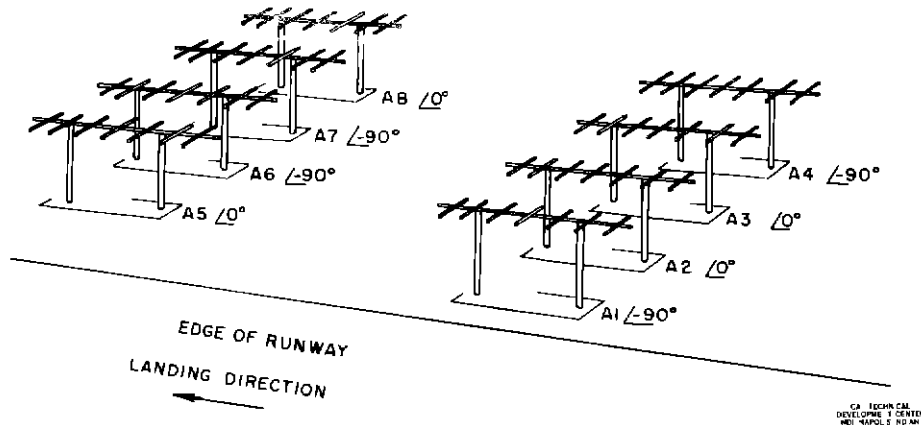


Fig 10 Pictorial Representation of Directional Glide Path Antenna System

The locus of point P for on-path indications would be a semicircle about the centerline of the antenna array. See Fig 8. This obviously is undesirable since a glide path of this type would provide the pilot correct vertical guidance only in the vertical plane which includes the centerline of the glide path antenna array or, what is very nearly the same plane, the vertical plane defined by the localizer. An ILS approach generally will involve some lateral error. Consequently, the glide path system must provide correct guidance over an area which has a width in azimuth at least comparable to the localizer course width. See Fig 9.

In order to provide a glide path having a width in azimuth comparable to the localizer course, namely, plus or minus  $2\frac{1}{2}^\circ$ , two broadside arrays of four elements each are employed in the directional glide path. The arrangement of the antenna system is shown in Fig 10. Also shown in the figure is the relative phasing of the currents supplied to the individual elements. The elements are identified in accordance with the following groups:

- A1 and A4 - outer pair, forward group
- A2 and A3 - inner pair, forward group
- A5 and A8 - outer pair, rear group
- A6 and A7 - inner pair, rear group

The horizontal spacing of the outer pair is 18.86 feet, or  $2,309.5^\circ$  at 335 Mc. The horizontal radiation pattern of this pair is shown in Fig 11. The spacing of the inner pair is 6.29 feet or  $769.8^\circ$  at 335 Mc. The horizontal radiation pattern of the inner pair is shown also in Fig 11. The patterns are symmetrical about the centerline of the system. Both pairs are fed with currents of equal amplitude. It is important to note that, along the centerline of the system, the amplitudes of the r-f fields of the inner and outer pairs are equal. As point P moves in azimuth at a constant elevation angle, the field intensity at point P varies as shown by the radiation patterns in Fig 11. For an angular departure of  $4.49^\circ$  from the centerline, the field contribution from the outer pair reduces to zero. At any azimuth angle, the total energy arriving at a point P consists of the sum of a component contributed by the outer pair and a component contributed by the inner pair. The ratio of the amplitudes of these components may be represented by R. R is a function of azimuth angle but not of elevation angle. The horizontal spacing between pairs of antennas may be adjusted such that the effect of relative phase shift of the r-f fields as point P moves horizontally at a constant elevation angle will be compensated for over a range of azimuth angle greater than the localizer course limits.

In describing the operation of the glide path system formed by the simple arrangement of an end-fire array, use was made of vector symbolism to show how the r-f field arriving at a point in space combined to produce the desired on-path, below-path, and above-path indications. The same procedure can be used to describe the operation of the glide path when

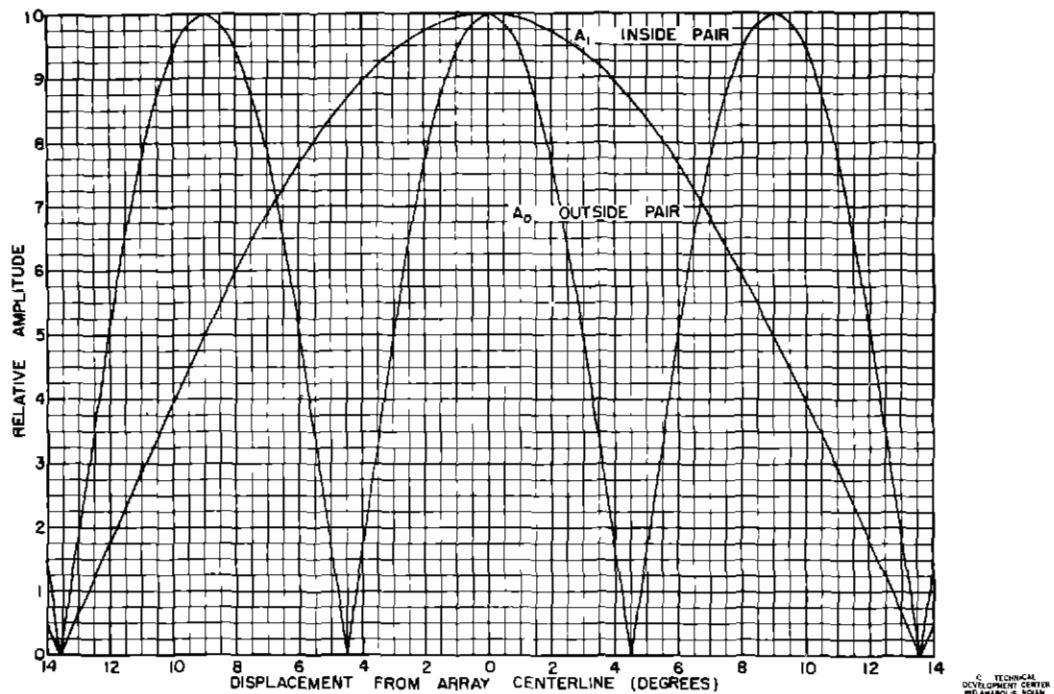


Fig 11 Horizontal Radiation Patterns of the Inner Pair and Outer Pair

the forward and rear antennas each are replaced by a broadside array of four elements. It will, however, make for a clearer explanation if a few concepts are fixed in mind and if a further simplification of the vector diagrams is tolerated. Accordingly, these concepts will be introduced and the justification for the form of the vector diagrams established.

Returning to the diagram in Fig 3, observe that the vector representation of the r-f field associated with a rear antenna element is similar in form to the vector representation of the r-f field associated with a forward element with one important difference. This difference lies in the position which the sideband vectors occupy, and is clearly shown in Fig 3. This is the only difference, and a simplification will be accomplished if the sideband vectors are deleted and a vector associated with the field from a rear element is distinguished by a dashed line. The field associated with a forward element will be represented by a solid line. It will be understood that a vector shown dashed includes the sidebands associated with a rear element (Fig. 3) and that a vector shown solid includes the sideband vectors which characterize the r-f field originating from a forward element. A further observation now can be made regarding the resultant when the r-f field from a forward element is combined with the r-f field from a rear element. If the dashed vector and the solid vector combine in phase, the resultant produces an on-path indication, if the dashed vector lags the solid vector, the resultant will produce a fly-up indication, and if the dashed vector leads the solid vector, the resultant will produce a fly-down indication. These three conditions are illustrated in Fig 12. If attention is confined to 0 to 90° of phase lead or lag, it is noted that the DDM, or the amplitude of the fly-up or fly-down indication, is a function of the amount of lead or lag. The relationship is very nearly linear and is shown in Fig. 13.

Returning now to the description of the behavior of the directional glide path employing a broadside array of four elements for the forward group and a broadside array of four elements for the rear group, it will be necessary to study the resulting r-f field in space at the point being considered. Four separate components are identified as follows:

- A1-A4 component originating from outer pair, forward group
- A2-A3 component originating from inner pair, forward group
- A5-A8 component originating from outer pair, rear group
- A6-A7 component originating from inner pair, rear group

The initial phasing is as represented in Fig. 10. The angles  $\theta$ ,  $\alpha$ , and  $\gamma$  are defined as shown in Fig 14.

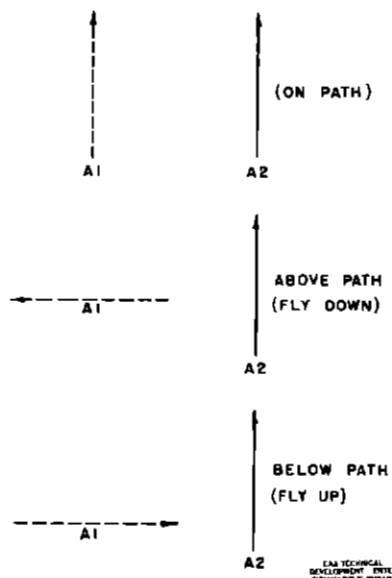


Fig 12 Simplified Vectorial Representation of RF Fields at Different Elevations

Consider the phase relationship of the r-f field as it arrives in space at a point along the centerline of the array ( $\theta$ ,  $\alpha$ , and  $\gamma$  all zero). The relative phasing of the two components associated with the inner and outer pairs of the forward group (A1-A4 and A2-A3) must remain at  $90^\circ$  since this is the initial phasing and the distance traveled by these components to arrive at a point along the array centerline is equal. The same is true of the phase relationship between the components of the field arriving from the inner and outer pairs of the rear group. However, the instantaneous phase relationship between the r-f field from the rear group and the forward group can be controlled by a phaser in the line feeding the rear group. It will help to visualize the effect of this control if it is regarded as a means of rotating the dashed vectors of Fig 15. If the control is moved in a direction to increase the length of the line feeding the rear group, the effect will be to rotate the dashed vectors in a clockwise direction, and if the control is moved in a direction to shorten the line length, the vectors move in a counterclockwise direction. Note that both vectors must move together, their relative position remaining fixed.

Next, consider a point in space located along the line for which  $\theta = 3^\circ$ ,  $\alpha$  and  $\gamma = 0^\circ$ . This point is on path and in the plane which includes the antenna system centerline. The instantaneous phase relationship between the r-f field from the forward and rear groups is controllable and this will be adjusted so that the arriving r-f field has the relationship shown in Fig 15.

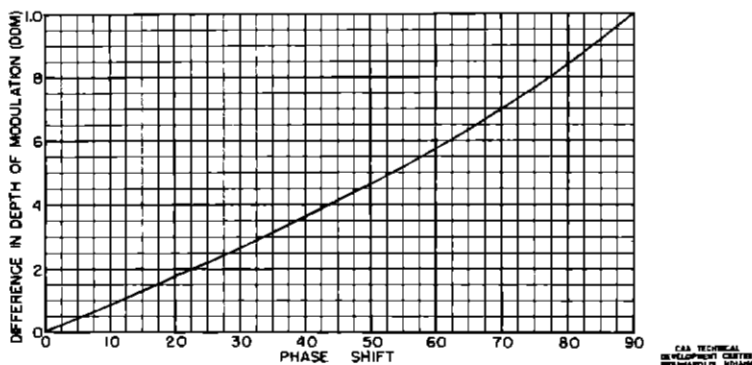


Fig 13 Difference of Depth of Modulation Versus Phase Shift

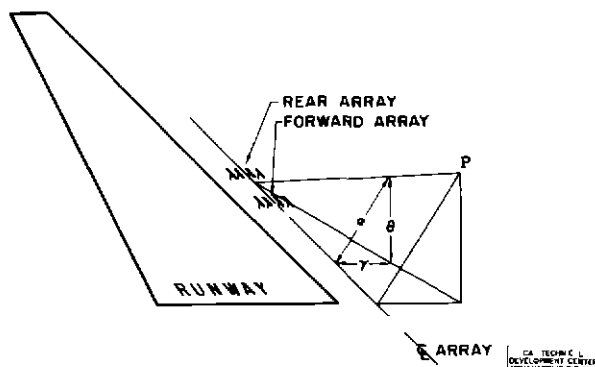


Fig 14 Pictorial Representation Illustrating Angles Involved

An inspection of Fig 15 shows that it satisfies the necessary conditions for an on-path indication. This can be verified by regarding the total field as the sum of two components. One of these components is the vector sum of A6-A7 and A1-A4. The other component is the vector sum of A5-A8 and A2-A3. Each of these two components is of a form which satisfies the requirement for on-path indication and it is concluded that the sum satisfies the requirement for on-path indication. Next, consider what happens when the point P moves above path in a plane which includes the centerline of the antenna system. This will have the effect of causing the dashed vectors to rotate counterclockwise. The vector diagram of Fig 16 illustrates the phase relationship of the r-f energy as it arrives at a point P above path. An inspection of this diagram shows that it will result in fly-down indication. This can be verified by reasoning similar to that used above. Regard A6-A7 and A1-A4 to be one component of the total energy arriving at P. Regard A5-A8 and A2-A3 as one component. Note that each of these components (A5-A8 plus A2-A3 or A6-A7 plus A1-A4) by themselves will contribute a fly-down indication. It is assumed that the sum satisfies the requirement for fly-down indication.

Now consider what happens when the point P moves along a line perpendicular to the centerline of the array. The horizontal radiation patterns of the inner and outer pairs will introduce an effect which is not present when P moves in the vertical plane. The vector diagram showing the phase relationship of the arriving r-f energy will have an appearance similar to the diagram for the case where P moved above path, but in addition to a phase rotation of the vectors, a change in amplitude will occur. This change in amplitude is the effect introduced by the horizontal patterns of the inner and outer pairs which, as previously mentioned, are a function of azimuth angle. An interesting case occurs when point P moves in azimuth sufficiently to cause a  $90^\circ$  phase change between the r-f fields arriving at P from the rear and forward antenna groups.

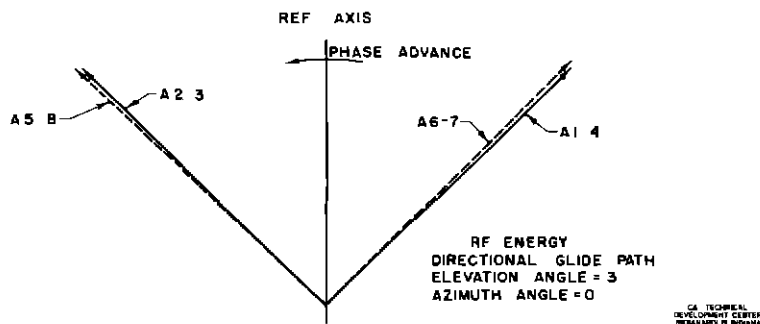


Fig 15 Vectorial Representation of "On-Path" Conditions

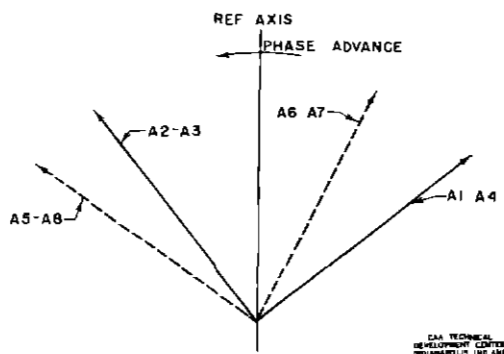


Fig 16 Vectorial Representation of "Above-Path" Conditions

A  $90^\circ$  phase change will result when P is displaced from a position where  $\theta = 3^\circ$  and  $\gamma = 0^\circ$  to a point where  $\theta = 3^\circ$  and  $\gamma = 4.49^\circ$ . This can be derived in the following manner

$$\alpha = \sqrt{\theta^2 + \gamma^2} \quad (1)$$

From small angles, the phase change can be calculated from the relation

$$\beta = s - s \cos \alpha \quad (2)$$

This is analogous to the method used to determine phase change when the motion of P was confined to a vertical plane which included the array centerline in which case  $\gamma$  was zero and the equation reduced to

$$\beta = s - s \cos \theta \quad (3)$$

For a spacing between the forward and rear antenna groups  $s = 29388^\circ$ , the phase change as P moves from a point at ground level to a position on path will be

$$\begin{aligned} \beta &= 29388 - 29388 \cos \alpha \\ &= 29388 - 29347^\circ \\ &= 41^\circ \end{aligned}$$

If P now moves in azimuth to a position where  $\theta = 3^\circ$  and  $\gamma = 4.49^\circ$ , the total phase change is

$$\begin{aligned} \beta &= s - s \cos 5.4^\circ \\ &= 29388 - (29388 \times 0.9956) \\ &= 131^\circ \end{aligned}$$

Observe that the phase change which results when P is displaced  $4.49^\circ$  in azimuth (from  $\theta = 3^\circ, \gamma = 0^\circ$  to  $\theta = 3^\circ, \gamma = 4.49^\circ$ ) is  $131^\circ - 41^\circ$  or  $90^\circ$

The vector diagram is shown in Fig 17. In constructing this diagram, it is noted that the phase shift is  $90^\circ$  and, consequently, the dashed vectors are rotated counterclockwise  $90^\circ$ . Since the motion is in azimuth, the amplitude also is affected. The amplitude of the two inner-pair vectors decreases from the reference amplitude of unity on the array centerline to a value of 0.87 at  $3^\circ$  from the centerline. The amplitude of the two outer-pair vectors reduces to zero. This accounts for the absence of the outer-pair vectors in Fig 17. This figure is particularly interesting since the contribution from the outer pair reduces to zero at the same time that the vectors representing the contribution from the inner pair coincide. This

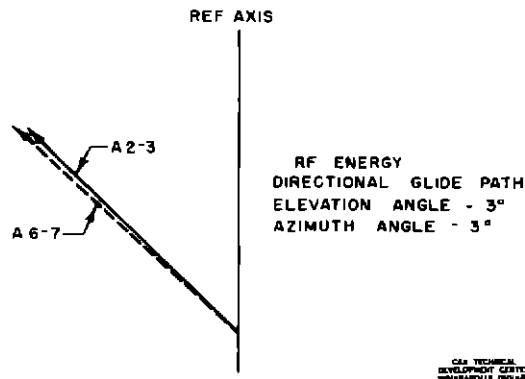


Fig. 17 Vectorial Representation for a Displacement of 3° from Array Centerline

condition of coincidence of inner-pair vectors defines on path and since it is the only resultant, the response at this azimuth angle is on path. This is a significant result since it has been shown that an on-path condition exists at path angle when  $\gamma = 0$  and at an azimuth angle of  $4.49^\circ$ .

## TEST RESULTS

### Description of Installation

A directional glide path was installed at the Kanawha County Airport, Charleston, West Virginia. The unusual terrain encountered at this airport is shown in Fig 18, which is a profile of the section along the runway centerline. The antenna system was essentially the same as described in the previous section. In the Charleston installation, however, both horizontal spacing and initial phasing were adjusted experimentally to those values which resulted in optimum performance.

At the Kanawha County Airport the instrument runway slopes downward toward the approach end at an angle of  $0.7^\circ$ . The desired inclination of the glide path was  $3.0^\circ$ . This necessitated adjustments of the antenna system to produce a path angle of  $3.7^\circ$ .

The centerline of the array was inclined  $2^\circ$  in azimuth toward the approach end of the runway to take advantage of the available width of the glide path which is approximately  $10.0^\circ$ , as shown in Fig 18A. This arrangement provides a glide path which is usable closer to touchdown than otherwise would be obtained if the centerline of the array was parallel to the

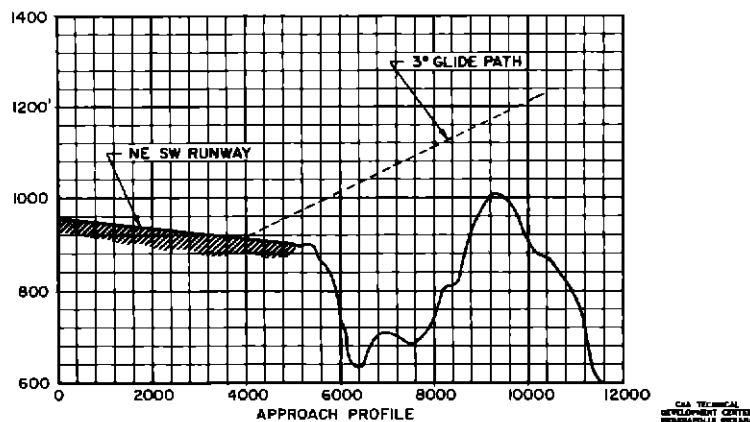


Fig 18 Approach Profile, Kanawha County Airport, Charleston, West Virginia

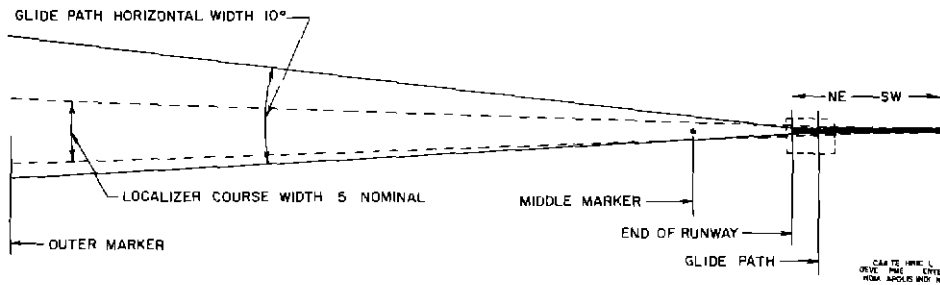


Fig 18A Plan View Showing Horizontal Width of Directional Glide Path

runway Figure 18B, which is an enlarged view of the area near touchdown, shows that when the aircraft on the approach is correctly aligned laterally (localizer needle centered), the glide path terminates when the aircraft reaches an altitude of approximately 30 feet above the runway Figure 19 shows the forward and rear groups of array elements and the monitor pickups of the Kanawha County Airport installation

#### Path Shape

After the antenna array was aligned properly and phased for optimum width in azimuth, a series of low approaches was flown in a DC-3 aircraft Figure 20A shows a typical recording of the CDI during an approach Along the margin of the recording are indicated the positions of the outer marker, the inner marker, and the approach end of the runway This type of recording is used frequently to establish the straightness of the path It is an indirect measure of path straightness since both turbulence and the pilot's proficiency affect the CDI indications However, it has been customary to define a path as acceptable when the recording of the CDI on a low approach shows excursions which do not exceed plus or minus 30 microamperes, or one dot <sup>4</sup> Using this interpretation, the recording of the low approach shown in Fig 20A would define a path that is acceptable regarding straightness It is, in fact, a fine approach, the excursions being confined to approximately plus or minus one-half dot

#### Vertical Path Width.

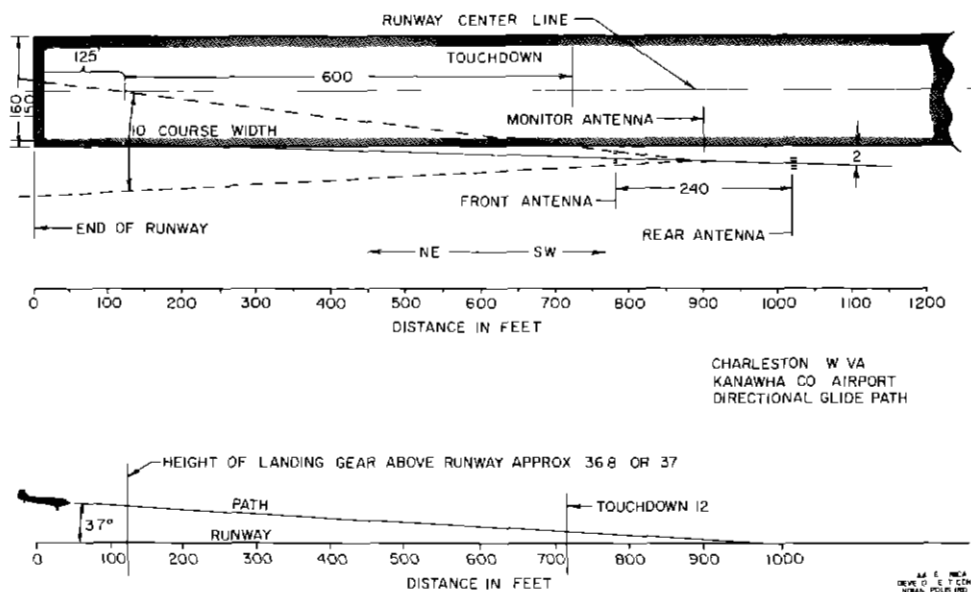
Figure 20B shows a recording of the CDI during level flight at 2,300 feet above mean sea level (MSL) toward the approach end of the runway and along the runway centerline This test and the resulting recording are used to measure path width in the vertical plane, clearance<sup>5</sup> beneath path, and general characteristics of the crossover The recording of Fig 20B shows that the clearance beneath the path is good, the crossover is uniform, and the course width in the vertical plane is 1.2° This course width is very nearly in the center of the limits established for course width

#### Horizontal Path Width

Figure 20C is a recording of the CDI when the aircraft was flown in level flight at 2,300 MSL perpendicular to the runway centerline and at a distance of approximately 4 1/2 miles from the approach end of the runway This recording gives a measure of the width of the course in azimuth On the margin of the recording is indicated the center of the localizer and its limits Since the localizer is nominally 5.0° in width, this provides a measure of the azimuthal width of the glide path, which is approximately 10.0°

<sup>4</sup>150 microamperes is equal to 5 dots

<sup>5</sup>Clearance is defined as the ratio, in db, of the 90-cps signal to the 150-cps signal, or vice versa, obtained after demodulation of the r-f field at any point in space by means of a linear detector.



### Measured Glide Path Data

From the flight tests at the Kanawha County Airport, the following data were calculated

Path Angle	-	$\angle 94^{\circ}$
Vertical Path Width	-	$\pm 0.635^{\circ}$
Horizontal Path Width	-	$\pm 4.5^{\circ}$
First False Path (path inverted)	-	$6.29^{\circ}$
Second False Path (path upright)	-	$8.52^{\circ}$





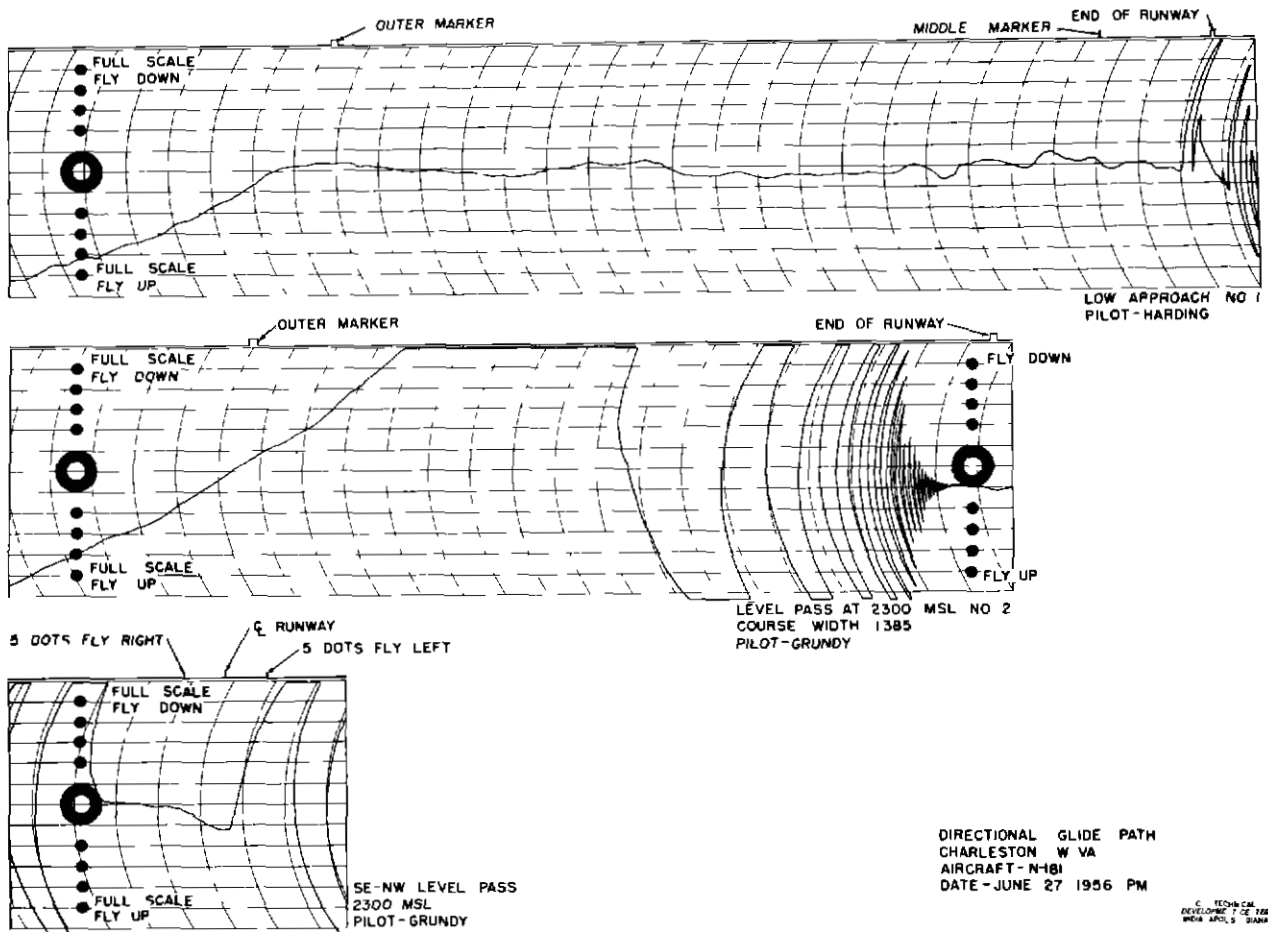


Fig 20 Recordings of Flight Test at Kanawha County Airport, Charleston, West Virginia

#### Importance of Phasing Stability

As previously explained, the path angle is determined by the initial phasing of the currents in the forward and rear antenna groups. In the actual installation, a phaser was inserted in the line supplying energy to the rear group. This phaser provides a convenient method for controlling path angle, and is very useful when making initial adjustments during installation. It can be used to vary path angle, including adjustment to an angle of  $0^\circ$ , which in turn allows measurement of path width by the use of ground equipment. This convenience of path adjustment, however, is obtained at a price. The stability of the path is dependent completely on the phase stability of the lines feeding the forward and rear antenna groups. During early experimental work, difficulty was encountered with the Type RG-8/U coaxial cable. This difficulty vanished when Styroflex cable was substituted for RG-8/U cable. Styroflex cable has substantially less loss and is much more stable than RG-8/U. The installation at Charleston was equipped with Styroflex cable. For approximately six months, path position remained within plus or minus  $0.07^\circ$ .

### THE MONITORING SYSTEM

#### Purpose

The monitoring system has several essential functions: detecting the presence of any malfunctioning, properly timing the equipment transfer, providing the control tower with both

visual and aural notice that a transfer has taken place, and shutting down the facility if transfer to standby equipment fails to correct the out-of-tolerance conditions

The monitor must check the radiations from all elements of the antennas continually and must provide an alarm whenever these radiations deviate from normal by a specified amount. The deviation limits are as follows:

1. A shift of path position above or below nominal by  $0.2^\circ$
2. A change in path width of  $0.4^\circ$
3. A reduction in power output to 50 per cent of normal

#### Principal Components.

The following equipments are the principal components of the monitor system. A brief description of each is included:

1. **Glide Path Monitor Type CA-1363.** The glide path monitor operating with its associated field detectors actuates an alarm circuit, and an automatic transfer circuit which places standby transmitter equipment in operation, whenever transmitted signals deviate from the specified limits.

Basically, the monitor consists of three channels described as follows:

- a. **Path Channel.** The path channel provides meter indications of the amplitudes of the 90- and 150-cps signal components from the output of the on-path field detector, and provides alarm indication when the ratio of the 90- to 150-cps signal components deviates from normal by a preset amount.
- b. **Modulation Level Channel.** The modulation level channel provides meter indication of the combined 90- and 150-cps amplitude from the output of the on-path field detector, and provides alarm indication when the combined level of the 90- and 150-cps signal components falls below a preset value.
- c. **Clearance Channel.** The clearance channel provides meter indications of the amplitudes of the 90- and 150-cps signal components from the output of the off-path field detector, and provides alarm indication when the ratio of the 90- to 150-cps signal components deviates from normal by a preset amount. The clearance channel also provides alarm indication when the combined level of the 90- and 150-cps signal components falls below a preset value.

The glide path monitor is contained in a single enclosed unit with door panel for mounting in a standard relay-rack cabinet. The height of the panel is 14 inches, the maximum depth behind the panel is 12 1/2 inches. The Type CA-1363 monitor is shown in Fig. 21.

2. **Glide Path Monitor Field Detector Type CA-1364.** Two field detectors are used with the glide path monitor to facilitate the detection of the on-path and off-path signals. The output of the on-path field detector actuates the path channel of the monitor, the output of the off-path detector actuates the clearance channel incorporated in the monitor. The field detector is designed for mounting on an upright support or pedestal in the field.

#### Operation of the Monitor

The two field detectors are located as shown in Fig. 22. The Yagi antennas of the glide path array are highly directional, and in order that the field detector can receive sufficient energy from each of the individual elements, it is necessary that the antenna of the field detectors be equipped with a reflector and a director to obtain the desired field pattern. Figure 23 is a view of the field detector installation.

The locations of the on-path field detector and the off-path field detector were determined experimentally, so that any phase or amplitude change in any one antenna of the directional glide path array which is sufficient to cause a change in path position or width exceeding designated tolerances will operate the monitor alarm.

The automatic transfer unit is operated by the monitor output. Upon receiving an alarm signal of greater than five seconds' duration, this unit switches the antenna array to a standby transmitter and a standby modulation unit. Simultaneously, an alarm signal is sent to the control tower to give both visual and aural notice that a transfer has taken place. If, after the changeover takes place, the alarm signal continues for five seconds, the facility is shut down. A further requirement of the monitor is that when power returns after a power failure,

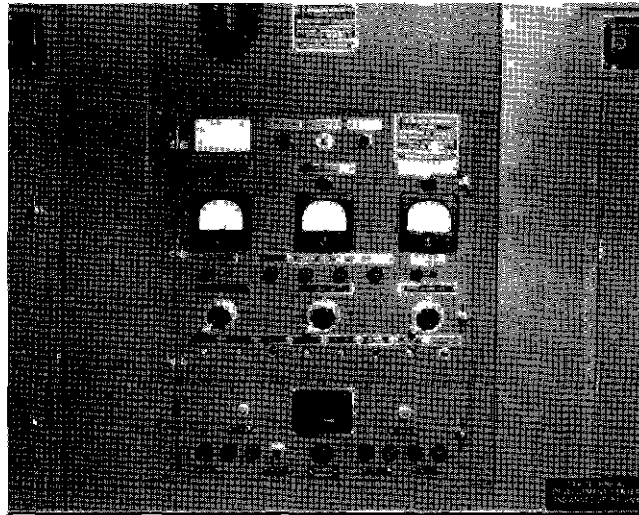


Fig 21 Glide Path Monitor Panel

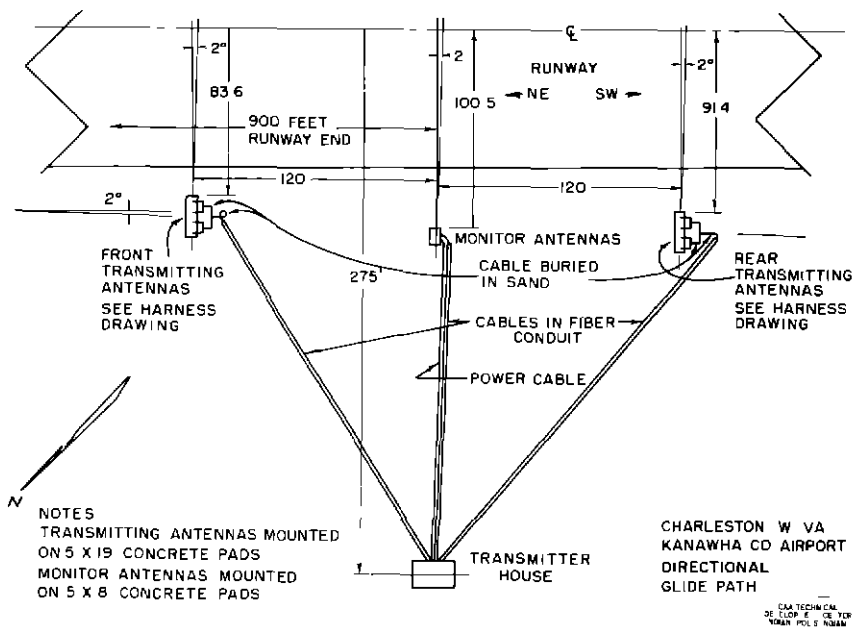


Fig 22 Physical Layout of Glide Path System



Fig 23 Monitor Field Detector

the monitor shall be prevented from giving an alarm until after the station and monitor equipment have had approximately one minute in which to warm up

The directional glide path array creates an unusual monitoring problem because of its proximity to the runway and the distance between the forward and rear arrays. If simple on-path and off-path field detectors were used, as in the case of the standard null-reference glide path, they would have to be located at a distance very much greater than the distance between the forward and rear arrays. Since this spacing is approximately 240 feet, the monitor location would have to be approximately 1,200 to 1,500 feet in front of the antenna system for the same sensitivity to a change in path configuration. This distance would make siting requirements most difficult.

#### Test Results

In order that variations in the path at 1,000 feet distance could be compared and correlated with the field detector indications, two telephone poles were erected temporarily 1,000 feet in front of the glide path array. One pole was placed on the centerline of the array. Half-wave dipoles were mounted on this pole at  $2.5^\circ$  (43.6 feet) and at  $2.0^\circ$  (35 feet) above the ground. The second pole was placed  $3.0^\circ$  in azimuth from the centerline of the array. A half-wave dipole was mounted on this pole at  $2.5^\circ$  (43.6 feet) above the ground. The dipoles were connected to standardized glide path receivers. A standardized glide path receiver produces a CDI deflection of 150 microamperes for an off-path deviation angle of  $0.75^\circ$ . Thus, the CDI deflection can be converted into change-of-path position in degrees, and can be used for calibration purposes. The monitor panel sensitivity controls are set to alarm when the path angle, as measured in the vertical plane which includes the runway centerline, is changed plus or minus 2 degrees by use of the phaser incorporated in the transmitters.

In order to determine the optimum positions of the on-path and off-path detectors, tests were made with a Type CA-1364 field detector, located 48 inches above ground, at intervals of 0, 3, 6, 9, and 12 feet perpendicular to the centerline and approximately midway between the front and rear arrays. It was determined from these tests that the optimum location for the on-path and off-path field detectors is at 6 feet and 12 feet, respectively, perpendicular to the centerline and approximately midway between the front and rear arrays. The field detectors were mounted on the side of the centerline of the system away from the runway.

A tabulation of the test data for the final location of the field detectors follows

## CONDITION I

An open transmission line to any one of the eight transmitting antennas

Antenna Number	Response as Measured in Space 1000 Feet Distant		Monitor Response		On-Path Modulation Level	Clearance Modulation Level
	0° Azimuth (degrees)	3° Azimuth (degrees)	On-Path (degrees)	Clearance (degrees)	(per cent)	(per cent)
1	+Full scale*	+Full scale*	<u>+0 36</u>	<u>-0 94</u>	195	108
2	-Full scale*	-0 68	<u>+0 88</u>	<u>+0 16</u>	112	114
3	-Full scale*	-Full scale*	<u>-0 34</u>	<u>-0 51</u>	<u>53</u>	<u>64</u>
4	+Full scale*	+0 41	<u>+1 56</u>	<u>+0 51</u>	126	97
5	+Full scale*	+Full scale*	<u>-0 32</u>	<u>-0 21</u>	<u>46</u>	<u>36</u>
6	-Full scale*	-Full scale*	<u>-0 45</u>	-0 02	88	75
7	-Full scale*	-Full scale*	<u>-0 82</u>	+0 01	76	<u>35</u>
8	+Full scale*	+Full scale*	<u>+0 76</u>	<u>-0 31</u>	118	172

\*Full scale indicates a deviation of 0 75 degrees or greater Underlined values indicate alarm condition (Path angle  $\pm 0 2$  degrees Modulation level below 70 )

## CONDITION II

A short-circuited line to any one of the eight transmitting antennas

1	+0 44	+Full scale*	<u>+0 78</u>	<u>-0 82</u>	157	122
2	-Full scale*	-Full scale*	<u>-0 22</u>	+0 17	<u>48</u>	77
3	-Full scale*	+Full scale*	<u>-1 68</u>	<u>-1 16</u>	128	91
4	+0 34	-0 22	<u>+0 83</u>	<u>+0 24</u>	74	70
5	+Full scale*	+Full scale*	<u>+0 69</u>	<u>+0 42</u>	80	86
6	-0 40	-Full scale*	<u>-0 98</u>	<u>-1.40</u>	90	75
7	-0 55	-0 18	<u>+0 49</u>	<u>+0 75</u>	<u>49</u>	142
8	+0 65	+0 37	<u>+0 82</u>	<u>-0 31</u>	162	176

\*Full scale indicates a deviation of 0 75 degrees or greater Underlined values indicate alarm condition (Path angle  $\pm 0 2$  degrees Modulation level below 70 )

## CONDITION III

Fifty-ohm dummy load substituted for any one of the eight transmitting antennas

Antenna Number	Response as Measured in Space 1000 Feet Distant		Monitor Response		On-Path Modulation Level	Clearance Modulation Level
	0° Azimuth (degrees)	3° Azimuth (degrees)	On-Path (degrees)	Clearance (degrees)	(per cent)	(per cent)
1	+Full scale*	+Full scale*	<u>+0 33</u>	<u>-0 82</u>	170	112
2	-Full scale*	-Full scale*	<u>-0 11</u>	<u>+0 37</u>	<u>56</u>	<u>84</u>
3	-Full scale*	-Full scale*	<u>-1 10</u>	<u>-0 77</u>	94	81
4	+Full scale*	+0 15	<u>+1 16</u>	<u>+0 40</u>	88	83
5	+Full scale*	+Full scale*	<u>+0 20</u>	<u>+0 22</u>	<u>59</u>	<u>55</u>
6	-Full scale*	-Full scale*	<u>-0 67</u>	<u>-0 59</u>	83	<u>55</u>
7	-Full scale*	-Full scale*	<u>+0 20</u>	<u>+0 11</u>	<u>57</u>	71
8	+Full scale*	+Full scale*	<u>+0 78</u>	<u>+0 39</u>	145	167

\*Full scale indicates a deviation of 0.75 degrees or greater Underlined values indicate alarm condition (Path angle  $\pm 0.2$  degrees Modulation level below 70 )

## CONDITION IV

Thirty-degree transmission-line extension inserted in the transmission line at any one of the eight transmitting antennas

1	-0 09	+0 50	<u>+0 69</u>	+0 09	102	112
2	-0 32	-0.43	<u>-0 43</u>	-0 19	102	93
3	-0.43	-0 88	<u>-0 49</u>	<u>-0 39</u>	124	106
4	-0 15	+0 45	<u>-0 22</u>	<u>-0 21</u>	74	88
5	+0 42	-0 14	<u>+0 38</u>	<u>+0 35</u>	103	101
6	+0 01	+0 37	+0 11	<u>+0 37</u>	76	84
7	+0 05	+0 25	<u>+0 25</u>	<u>+0 26</u>	89	112
8	+0 44	+0 42	-0 11	<u>-0.56</u>	127	93

\*Full scale indicates a deviation of 0.75 degrees or greater Underlined values indicate alarm condition (Path angle  $\pm 0.2$  degrees Modulation level below 70 )

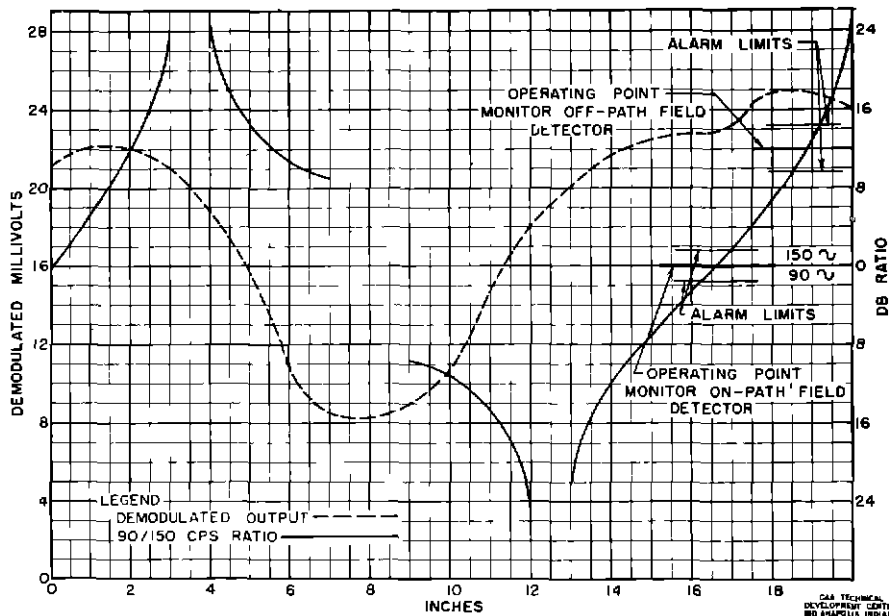


Fig 24 Data From Monitor Field Detector for Determination of Monitor Field Detector Positioning

It will be noted that when the on-path field detector was placed 6 feet from the centerline and adjusted fore and aft for 0 db 90/150-cps ratio and the off-path field detector was placed 12 feet from the centerline and adjusted fore and aft for 12 db 150/90-cps ratio, at a position where the carriers were in phase, all simulated conditions of malfunctioning showed the monitor to be approximately as sensitive to the variations as the receivers were on path at 1,000 feet

Data obtained by moving the field detector forward along a line 12 feet from and parallel to the centerline are plotted in Fig 24. Both the demodulated output and the 90/150-cps ratios versus distance in inches are shown. It can be seen from the alarm limits that the position of the field detectors must be rigidly fixed in the front and rear directions. In order that ground freezing and thawing would not affect these positions, each of the detectors was supported by a two-inch aluminum pipe and frangible coupling mounted on a concrete base which extended below the frost line.

Tests were conducted to simulate the effect of a large bird perched on the end of one of the elements of a field detector. A large wet cloth was substituted for the bird on the end of a dipole and reflector. The presence of the wet cloth caused a large change in both the amplitude and the 90/150-cps ratio as indicated by the monitor. The information obtained from this test showed that it was necessary to provide protection over the entire field detector antenna. Covers made of fiberglass were found to provide satisfactory protection.

Tests also were conducted to determine the effect a change in power level to each antenna array would have on path width and monitor indications. Flight-test data and monitor indications for a change in power to the rear antenna array are tabulated below.

Power in Rear Array (watts)	Attenuation (db)	Measured Course Width (degrees)	Monitor On-Path		Monitor Clearance		Monitor Modulation Level (per cent)
			90-cps	150-cps	90-cps	150-cps	
4.6	0	1.086	100	100	100	100	100
2.2	3.2	1.278	74	74	62	73	71
0.9	7.08	1.376	46	49	25	54	58

As shown in the above data, a 7.08-db attenuation between the front and rear antenna arrays spreads the path by  $0.29^\circ$ . The same attenuation caused the on-path monitor readings of 90 and 150 cps to show a difference of 0.5 db and the clearance monitor readings to show a difference of 6.7 db. Neither of these differences is sufficient to cause an alarm, however, the on-path modulation level meter reading showed a decrease of 4.7 db, which was sufficient to cause an alarm.

To test the effect of a large reflecting object near the array, a Douglas DC-3 airplane was taxied, turned around, and parked on the runway opposite the center of the array. The maneuver caused no alarm. A Lockheed Constellation aircraft, whose wings extend out farther than the DC-3, caused intermittent and very short duration alarm conditions during taxi, takeoff, and landing. Trucks and personnel moving about in the area between the transmitting antenna and the monitor field detectors caused an alarm condition.

Tests were conducted to determine the effect of a steel ground mat at various distances from the monitor field detector. It was found that the effect was greatest near and under the detectors and less as the mat was moved farther toward the front or rear arrays. The stability of the field detectors appeared to improve by the use of a 30-foot diameter steel ground mat immediately under and about the detector.

During service tests at Kanawha County Airport, Charleston, West Virginia, a ground mat similar to the above was found necessary. During a sudden rain squall, it was found that the ground condition varied enough to cause an alarm due to amplitude change in the received demodulated signals.

In the description of the directional glide path operation, it was shown that the glide path has a usable limit in azimuth somewhat greater than plus or minus  $5.0^\circ$ . Beyond the  $5^\circ$  departure from the array centerline, the locus of points is characterized by equal 90- and 150-cps modulation from a line which intersects the ground at approximately  $6.5^\circ$ . On the Kanawha County Airport, the area at about  $6.0^\circ$  from the antenna centerline and 1,500 feet from the antenna is easily accessible for the installation of measuring equipment. Equipment was installed at this location for collecting data on the stability of the path position and on-path width.

The equipment installation at this site consisted of

- 1 Two antenna pickups supported on poles about 12 feet above the ground
- 2 A small shelter equipped with a regulated a-c power supply, which housed a standardized glide path receiver, a d-c amplifier, and an Esterline-Angus graphic recorder

One of the antenna pickups was adjusted horizontally until a location was found where the received signal gave an on-path indication when connected to the standardized glide path receiver and when the path in space was set at  $3.0^\circ$ . The other antenna was adjusted horizontally to a position where its output, when connected to a standardized glide path receiver, gave approximately 100 microamperes fly-down indication. The lines from the two antennas were terminated in a single-pole, double-throw coaxial switch so that their outputs could be applied alternately to the standard glide path receiver.

The above equipment at the described location provided the means for obtaining a continuous recording of the path position, and this recording could be interrupted by the manual operation of the coaxial switch to obtain a measure of path width. The data collected indicated that the path position for the first six months after the installation remained within plus or minus  $0.07^\circ$  of its initial setting.

## CONCLUSIONS

1 The results of the tests of the directional glide path at the Kanawha County Airport, Charleston, West Virginia, are very encouraging. A straight path was produced at a site where previous attempts with both the null-reference and equisignal-type systems failed. Since the Charleston site is an example of extremely rough terrain, it is concluded that the directional glide path can provide a straight path at similar sites where the terrain is very rough.

2 The long-term stability of path position is acceptable. During the stability tests of the installation at the Charleston site, the usual wide temperature, rainfall, and humidity ranges for this area were encountered and path position was well within stability limits.



3 The directional glide path provides a path which terminates essentially when the aircraft reaches an altitude of approximately 30 feet above the runway, on the localizer course. This is entirely adequate for the operational use that is made of the ILS at this time.

4 The monitor system described provides adequate protection against typical faults that might occur in the glide path array.